International Journal of Biochemistry and Cell Biology 113 (2019) 75–86

Contents lists available at ScienceDirect

International Journal of Biochemistry and Cell Biology

journal homepage: www.elsevier.com/locate/biocel

The RNA-binding protein SRSF1 is a key cell cycle regulator via stabilizing NEAT1 in glioma

Xuexia Zhou[a,b,c], Xuebing Li[d], Lin Yu[e], Run Wang[a,b,c], Dan Hua[a,b,c], Cuijuan Shi[a,b,c], Cuiyun Sun[a,b,c], Wenjun Luo[a,b,c], Chun Rao[a,b,c], Zhendong Jiang[a,b,c], Qian Wang[a,b,c], Shizhu Yu[a,b,c,*]

[a] Department of Neuropathology, Tianjin Neurological Institute, Tianjin Medical University General Hospital, Tianjin, China
[b] Tianjin Key Laboratory of Injuries, Variations and Regeneration of the Nervous System, Tianjin, China
[c] Key Laboratory of Post-trauma Neuro-repair and Regeneration in Central Nervous System, Ministry of Education, Tianjin, China
[d] Tianjin Key Laboratory of Lung Cancer Metastasis and Tumor Microenvironment, Tianjin Lung Cancer Institute, Tianjin Medical University General Hospital, Tianjin, China
[e] Department of Biochemistry and Molecular Biology, School of Basic Medical Sciences of Tianjin Medical University, Tianjin, China

ARTICLE INFO

Keywords:
Glioma
SRSF1
Cell cycle progression
NEAT1
RNA stability

ABSTRACT

The relevance of RNA processing has been increasingly recognized in a variety of diseases. We previously identified serine/arginine-rich splicing factor 1 (SRSF1) as an oncodriver in glioma via splicing control. However, its splicing-independent roles and mechanisms are poorly defined in glioma. In this study, by integrating the data mining of *SRSF1*-co-expressed genes, SRSF1-affected genes and experimental studies, we demonstrated that *SRSF1* was the most highly expressed *SRSF* in the 9 tumor types tested, and it was a crucial cell cycle regulator in glioma. Importantly, we identified nuclear paraspeckle assembly transcript1 (*NEAT1*), an upregulated long non-coding RNA (lncRNA) in glioma, as a target of SRSF1. Endogenous *NEAT1* inhibition resembled the effect of SRSF1 knockdown on glioma cell proliferation by retarding cell cycle. Mechanistically, we proved that SRSF1 bound to *NEAT1* and facilitated its RNA stability. The positive correlation between *SRSF1* and *NEAT1* levels in cancers further supported the positive regulation of *NEAT1* by SRSF1. Collectively, our results provide novel insights on the splicing-independent mechanisms of SRSF1 in glioma, and confirm that *NEAT1*, whose stability maintained by SRSF1, implicates gliomagenesis by regulating cell cycle. Both SRSF1 and *NEAT1* may serve as promising targets for antineoplastic therapies.

1. Introduction

Gliomas are the most common primary tumors in the central nervous system (Louis et al., 2016). Malignant glioma, for instance, glioblastoma (GBM), is featured by rapid growth and relentless infiltration, which makes complete tumor resection almost impossible (Lara-Velazquez et al., 2017). Despite the considerable advances in neuro-oncology in the last few decades, the clinical outcome of GBM patients remains largely unsatisfactory (Alexander and Cloughesy, 2017).

RNA-binding proteins (RBPs) are master regulators on RNA fate from synthesis to decay, including RNA processing (splicing, capping and polyadenylation), transport, degradation and translation (Castello et al., 2012). They regulate gene expression in a post-transcriptional manner and are involved in various cellular phenotypes (Conlon and Manley, 2017; Masuda and Kuwano, 2018; Moore and von Lindern, 2018). Alterations in RBPs due to mutation, copy number variation or else are frequently observed in human cancers, and abnormal RBP expression also contributes to tumorigenesis via regulation on gene/protein homeostasis (Hong, 2017; Pereira et al., 2017).

Serine/arginine-rich splicing factor 1 (SRSF1) belongs to the splicing factor category of RBPs. It is overexpressed and functions as an onco-protein in numerous malignancies (Das and Krainer, 2014). Our previous study has described its oncogenic roles in glioma, including facilitating cell proliferation, survival and invasion via alternative splicing (AS) control of myosin IB (*MYO1B*) gene (Zhou et al., 2019). Cell cycle arrest or process is the major switch resulting in cell proliferation inhibition or promotion, respectively (Besson and Yong, 2001; Evan and Vousden, 2001). Two classes of regulatory molecules,

* Corresponding author at: Department of Neuropathology, Tianjin Neurological Institute, Tianjin Medical University General Hospital, 154 Anshan Road, Tianjin 300052, China.
E-mail address: tjyushizhu@163.com (S. Yu).

https://doi.org/10.1016/j.biocel.2019.06.003
Received 9 February 2019; Received in revised form 4 June 2019; Accepted 10 June 2019
Available online 11 June 2019
1357-2725/

cyclins and cyclin-dependent kinases (CDKs), are key deciders of cell cycle progression. However, whether SRSF1 accelerates glioma cell proliferation via cell cycle control remains unknown. Apart from AS, SRSF1 also participates in other RNA processing processes, such as RNA transcription, stability and nuclear export (Das and Krainer, 2014; Martinez-Terroba et al., 2018). Nevertheless, whether its splicing-independent mechanisms are implicated in gliomagenesis stays unclear.

Long non-coding RNAs (lncRNAs) are a prominent class of RNAs sized over 200 nucleotides with no protein coding capacity. They are involved in various biological processes via controlling gene/protein expression, stability and activation (Balas and Johnson, 2018; Rafiee et al., 2018). Dysregulation of lncRNAs engages in tumorigenesis, and lncRNAs emerge as novel biomarkers and therapeutic targets for glioma (Peng et al., 2018; Shi et al., 2017). Nuclear paraspeckle assembly transcript1 (*NEAT1*) is a nuclear enriched lncRNA containing two transcripts, *NEAT1_1* (3.7 kb; stabilized by poly-A tail) and *NEAT1_2* (23 kb). Scholars have demonstrated the essential oncogenic nature of *NEAT1* in many malignancies, including in glioma (Klec et al., 2018; Zhou et al., 2018). Nonetheless, the relationship between *NEAT1* and RBPs remains poorly understood.

In the present study, we reiterated the overexpression of SRSF1 in gliomas. Combining the in silico analysis results of *SRSF1*-co-expressed genes, the RNA-seq data derived from SRSF1-silenced cells and solid experimental data, we verified that SRSF1 promoted GBM cell proliferation by facilitating cell cycle (G1) progression. Moreover, this promotion on GBM cell proliferation was linked with the stabilizing of *NEAT1* by SRSF1. Our findings propose a splicing-independent modulation of SRSF1 through controlling the RNA stability of *NEAT1* in GBM cells.

2. Materials and methods

2.1. In silico analysis of SRSF expression in pan-cancer and SRSF1-co-expressed genes

We analyzed the tumor expression profile of *SRSF* genes (*SRSF1-10*) across the human RNA-seq compendium comprising 9 tumor types and 1023 samples using the Anatomy tool of Genevestigator v3 (NEBION, Zurich, Switzerland) (Hruz et al., 2008). cBioPortal (http://www.cbioportal.org) was applied to screen the *SRSF1*-co-expressed genes in GBM. The selection threshold was defined as the absolute value of Spearman's correlation coefficient > 0.5. Protein products of the screened 360 co-expressed genes were then adopted to map the interaction network and analyze the function enrichment using STRING (http://string-db.org).

2.2. Tissue samples and clinical data

Resected specimens of 30 astrocytic gliomas and 5 non-tumoral brain tissues (control) were collected from Tianjin Medical University General Hospital (TMUGH). Specimens are pathologically graded according to the 2016 World Health Organization (WHO) criteria. The baseline clinical features of the included patients were available in Supplementary Table 1. For histological analysis, specimens were immediately fixed in 3.7% buffered formaldehyde solution after surgical excision and embedded in paraffin afterwards. Then, 5 μm continuous sections were prepared for immunohistochemistry (IHC) of SRSF1. Another repeats of tissues were preserved in liquid nitrogen and stored at −80 °C until used for RNA extraction. This study has been approved by the Ethics Committee of TMUGH, and all participants signed informed consent.

2.3. Cell culture and reagents

Human GBM cell lines, U87MG cells were obtained from the American Type Culture Collection (ATCC, Manassas, VA, USA). LN229, U251, U343 and SNB19 cells were purchased from the China Academia Sinica Cell Repository (Shanghai, China). The GBM cell line TJ905 from a Chinese patient was established and maintained by our lab. The immortalized human astrocyte cell lines (UC2 and UC3) were used as non-tumoral controls. All the cell lines were maintained in Dulbecco's Modified Eagle Medium (DMEM; Gibco, Grand Island, NY, USA) supplemented with 10% fetal bovine serum (FBS; Gibco), 100 U/mL penicillin and 100 mg/mL streptomycin at 37 °C in a humidified atmosphere containing 5% CO_2. Actinomycin D (ActD) was ordered from Medchemexpress (MCE, Shanghai, China).

2.4. SiRNAs, plasmids, lentiviruses and stable sub-cell line establishment

SiRNAs targeting SRSF1 and *NEAT1* were ordered from GenePharma (Suzhou, China) and transfected with Lipofectamine RNAiMAX (Invitrogen, Carlsbad, CA, USA). Plasmid expressing the *NEAT1_1* (3756 bp) transcript was constructed in pCMS-EGFP vector. Plasmid expressing HA-tagged SRSF1 was constructed in pcDNA3.0 vector. Plasmid transfection was performed using X-tremeGENE HP DNA Transfection Reagent (Roche, Indianapolis, IN, USA). The recombinant lentiviruses expressing sh-SRSF1, sh-*NEAT1* and negative control sh-NC were generated with PLKO.1-puro lentiviral vectors in 293 T cells. Stable sub-cell lines were established by infecting with the indicated lentiviruses and selected for puromycin resistance. Sequences of the abovementioned siRNAs, shRNAs and cloning primers were listed in Supplementary Table 2.

2.5. RNA extraction, qPCR, RNA immunoprecipitation (RIP) and RT-PCR

RNA extraction and reverse transcription (RT) were carried out as described previously (Zhou et al., 2017). qPCR was performed with the GoTaq qPCR Master Mix Kit (Promega, Fitchburg, WI, USA) and *β-actin* was used as the internal control. Fold changes of target gene expression were calculated by the $2^{-\Delta\Delta Ct}$ method. RIP assay was performed as previously described (Zhou et al., 2014a). Cell lysates were incubated with the HA tag antibody (catalog ab9110, Abcam, Cambridge, MA, USA) for 6 h in 4 °C. RNA was extracted from the immunoprecipitate and cDNA was synthesized with random primers. RNA enrichment was detected by RT-PCR. qPCR and RT-PCR primers were synthesized by Beijing Genomics Institute (BGI, Beijing, China) and listed in Supplementary Table 3.

2.6. IHC and Western blot

IHC was performed with the mouse anti-human SRSF1 (catalog sc-33652; Santa Cruz Biotechnology, Santa Cruz, CA, USA) antibody as previously described (Liu et al., 2015). Western blot was performed as previously described (Li et al., 2017a). The following commercially available antibodies were purchased from Santa Cruz Biotechnology: SRSF1 (catalog sc-33652), β-actin (catalog sc-47778), Cyclin D1 (catalog sc-70899) and CDK2 (catalog sc-6248). The following antibodies were purchased from Cell Signaling Technology (Boston, MA, USA): Cyclin E2 (catalog 4132) and CDK6 (catalog 13331).

2.7. Cell viability and cell proliferation assays

Cell viability was assessed by crystal violet staining as previously described (Li, X. et al., 2017). Briefly, cells seeded in six-well plates were fixed in 4% paraformaldehyde, washed with PBS twice, and stained with 0.1% crystal violet solution for 30 min at room temperature. Cell proliferation was measured by 5-ethynyl-2′-deoxyuridine (EdU) staining as previously described (Li et al., 2017a).

2.8. Cell cycle analysis

Cell cycle was determined by propidium iodide (PI) staining as

previously described (Li et al., 2017b). In brief, cells were harvested and fixed with 70% ice-cold ethanol at −20 °C overnight. Then cells were stained by 50 μg/mL of PI staining buffer containing 0.1% TritonX-100 and 200 μg/mL of RNaseA for 30 min at 37 °C. Flow cytometry was finished with the Accuri C6/FACSCalibur Flow Cytometer (BD Biosciences, Franklin Lakes, NJ, USA). ModFit software (Verity Software House, Topsham, ME, USA) was employed for data analysis.

2.9. Intracranial xenograft assay in nude mice

Female BALB/C athymic nude mice (4 weeks old) were from the animal center of the Cancer Institute of Chinese Academy of Medical Science (Beijing, China). The indicated cell cultures of stable sub-cell lines were transplanted intracranially (3×10^5 cells per mouse) as described previously (Zhou et al., 2019). The intracranial tumor growth was monitored by bioluminescence imaging every week post transplantation (day 5, 12, 19, 26).

2.10. RNA-seq and data analysis

Total RNA isolated from control (sh-NC) or SRSF1 knockdown (sh-SRSF1) groups of U87MG and U251 cells were subjected to paired-end RNA-Seq using Illumina HiSeq 2000 system. Reads mapping and data analysis for differential expressed genes were carried out as previously described (Zhou et al., 2014b). The raw sequence data has been submitted to Gene Expression Omnibus with accession number 109,436. Volcano plots, Venn diagrams and heatmaps for differential expressed coding and non-coding RNAs were drawn by R language. The functional protein interaction network, KEGG pathway and gene ontology (GO) enrichment analyses for the overlapping differential expressed coding genes in U87MG and U251 cells were accomplished by STRING.

2.11. Microarray analysis

Expression profiles of the selected lncRNAs were established by microarray analysis on the basis of the published data of Bredelet al (Bredel et al., 2006) which profiled gene expression in 50 glial brain tumors and 4 normal brains by 42,000-feature cDNA microarrays. The 50 glioma specimens including 8 oligodendrogliomas, 6 anaplastic oligoastrocytomas tumors, 31 glioblastomas and 1 glioneuronal neoplasm were subjected to standard WHO classification. These data were downloaded from the GEO datasets under accession number GDS1813 (https://www.ncbi.nlm.nih.gov/gds). Expression of the selected lncRNAs was displayed by heatmap.

2.12. Statistics

Data were disposed as the mean ± standard deviation (SD). Statistical analyses were performed using SPSS 21.0 software (IBM, Chicago, Illinois, USA). Student's *t* test, 1-way ANOVA test and Pearson correlation analysis were used to analyze the corresponding data. Statistical significance was assigned at $P < 0.05$ (*), $P < 0.01$ (**) or $P < 0.001$ (***). All the experiments of cell lines were performed at least three times with triplicate samples.

3. Results

3.1. SRSF1 overexpression in glioma and its co-expression gene network analysis

To evaluate the implication of SRSF genes in tumorigenesis, we firstly dissected the expression profile of *SRSF* genes (*SRSF1-10*) in 9 tumor types including 1023 samples using the Anatomy tool of Genevestigator v3. In silico analysis revealed that *SRSF1* was the most highly expressed *SRSF* gene in the tumors, including in glioma (Fig. 1a). Notably, *SRSF2*, *SRSF3*, *SRSF9* and *SRSF10* also exhibited highly expression in these tumors, suggesting their potential roles in tumorigenesis (Fig. 1a). Subsequent IHC confirmed the upregulation of SRSF1 in gliomas, and its labeling indexes progressively increased along with the elevation of glioma grades (Fig. 1b). Western blot showed that SRSF1 was increased in most of the GBM cell lines (5/6) compared with that in the immortal human astrocyte cell lines UC2 and UC3 (Fig. 1c).

To comprehensively understand the role of SRSF1 in GBM, we screened the *SRSF1*-co-expressed genes through cBioPortal by setting the absolute value of Spearman's correlation coefficient > 0.5. A total of 360 genes were then submitted to STRING to construct the protein-protein interaction network (Fig. 2a). KEGG pathway and GO analyses verified that *SRSF1*-co-expressed genes were markedly enriched in cell cycle regulation (Fig. 2b). These results collectively indicate the critical role of SRSF1 in glioma possibly via cell cycle regulation.

3.2. SRSF1 knockdown inhibits GBM cell proliferation and cell cycle progression

We have proved that SRSF1 is crucial for glioma cell proliferation, survival and invasion previously (Zhou et al., 2019). To examine the contribution of SRSF1 in cell cycle control to the proliferation phenotype of GBM cells, we performed loss-of-function studies in U87MG and U251 cells. qPCR and Western blot confirmed the knockdown efficiencies of small interfering RNAs (siRNAs) targeting SRSF1 (Fig. 3a, b). Cell viability and proliferation, determined by crystal violet staining and EdU assay, respectively, was significantly inhibited by SRSF1 knockdown compared with control cells transfected with a negative control siRNA (NC-si; Fig. 3c, d). Furthermore, cell cycle analysis by flow cytometry revealed that SRSF1 knockdown resulted in significant G1 arrest, which might explain the growth-inhibitory effects of SRSF1-siRNAs in U87MG and U251 cells (Fig. 3e). These data support that SRSF1 is a potent promoter of glioma cell proliferation at least partially through cell cycle regulation, which is in line with the above findings from its co-expression gene network analysis.

3.3. RNA-seq identifies SRSF1 as a cell cycle regulator and NEAT1 as its candidate target

Previously we conducted high throughout sequencing of RNA (RNA-seq) on the control (sh-NC) and SRSF1 knockdown (sh-SRSF1) groups of U87MG and U251 sub-cell lines (GEO109436). Besides the identification of numerous AS events affected by SRSF1, we also observed the effects of SRSF1 on global gene expression (Zhou et al., 2019). Specifically, for those differential expressed coding mRNAs affected by SRSF1 knockdown in U87MG and U251 cells (Fig. 4a), we focused on the overlapping ones (Fig. 4b) shared by the two cell lines, since they might reflect the generality of gliomagenesis regulated by SRSF1. Importantly, these overlapping SRSF1-activated coding genes (downregulated genes in SRSF1-silenced cells) were enriched in the cell cycle control and other basic biology processes like DNA replication, DNA repair and cell division (Fig.4c, d). Moreover, Gene Set Enrichment Analysis (GSEA) showed that SRSF1 expression positively correlated with the E2F targets and G1/S checkpoint gene signatures (Supplementary Fig. 1).

Since our RNA-seq libraries were prepared from total RNA using poly-A enrichment of the mRNA, we could also detect the existence of non-coding RNAs (ncRNAs) with poly-A tails. Similarly, we observed that SRSF1 knockdown induced differential expression of a cohort of ncRNAs, which could be classified into five major categories (Fig. 5a, b). Heatmap of the differential expressed lncRNAs affected by SRSF1 knockdown exhibited both generality and specificity between U87MG and U251 cells (Fig. 5c). We further sorted out a list of common lncRNAs regulated by SRSF1, including 8 downregulated and 6 upregulated lncRNAs from all the differential expressed lncRNAs (Fig. 5d). Among these common lncRNAs, *NEAT1_1* (abbreviated as *NEAT1* below), a well-known oncogenic lncRNA, attracted our attention. qPCR

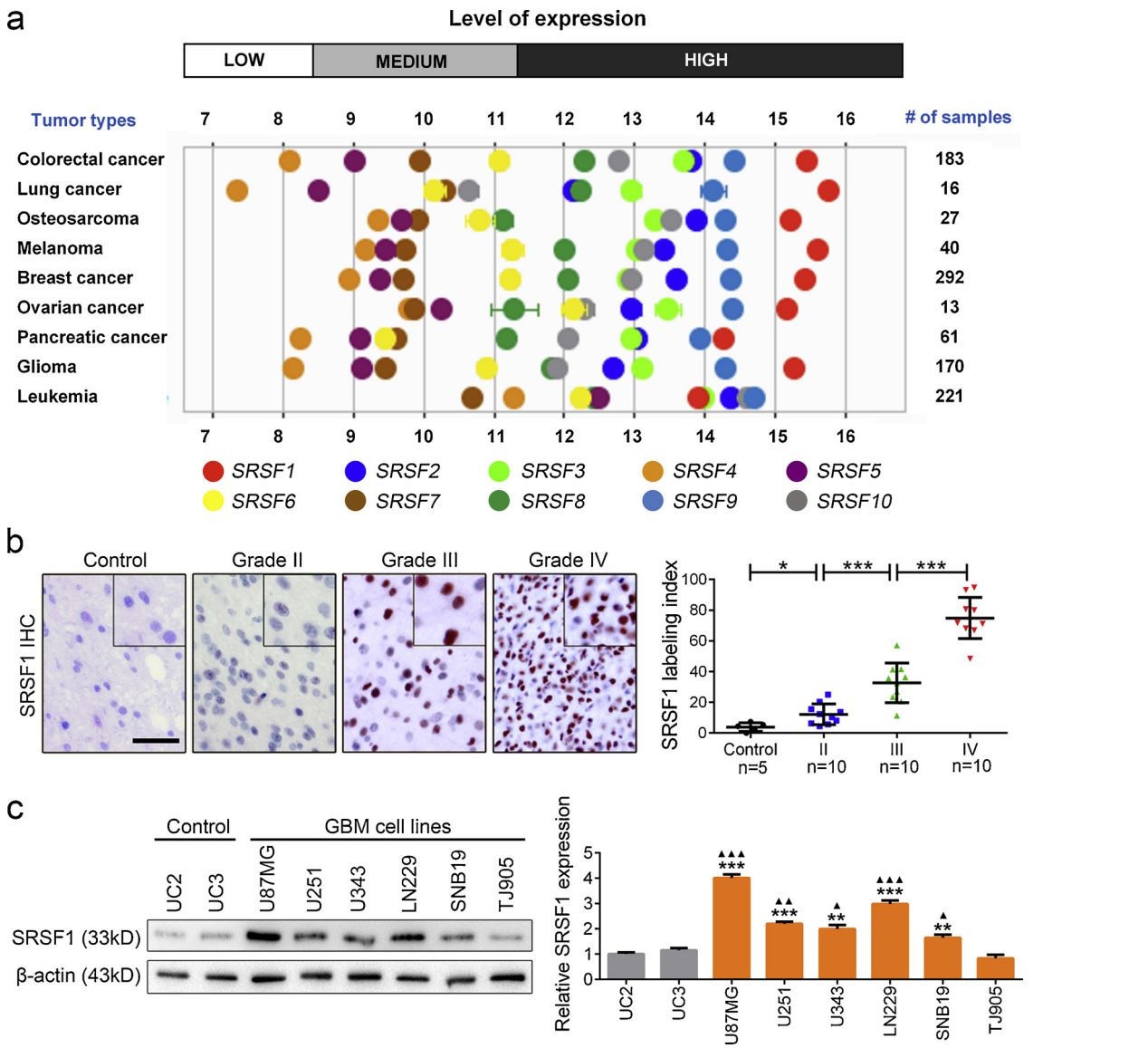

Fig. 1. Highly expression of SRSF1 in GBM. (a) Expression profile of *SRSF* genes (one probe for each gene) in 9 human tumor types plotted by Genevestigator. *SRSF1* represents as the most highly expressed *SRSF* in tumors, including in glioma. (b) Representative IHC staining for SRSF1 in graded gliomas (left) and quantification of SRSF1 expression levels [Labeling index (%)] among groups of the FFPE samples (right). Scale bar, 30 μm. Data are presented as the mean ± SD. $^{*}P < 0.05$, $^{***}P < 0.001$. (c) Western blot (left) and quantification (right) of SRSF1expression in GBM cell lines compared with the immortalized human astrocyte cell lines UC2 and UC3. Loading control: β-actin. Data are presented as the mean ± SD. $^{**}P < 0.01$, $^{***}P < 0.001$ vs. UC2; ▲ < 0.05, ▲▲ < 0.01, ▲▲▲ < 0.001 vs. UC3.

validated that SRSF1 knockdown inhibited *NEAT1* expression, which was consistent with the RNA-seq data (Fig. 5e).

3.4. Upregulated NEAT1 in glioma promotes cell proliferation and cell cycle progression

To our knowledge, scholars have already documented *NEAT1* up-regulation in several cancers, including in glioma (Klec et al., 2018; Zhou et al., 2018). We now analyzed the expression of the common lncRNAs regulated by SRSF1 on the basis of the published data (GDS1813). Importantly, *NEAT1* levels revealed by four independent probes exhibited regularly upregulation in GBMs, comparing with that in normal brains and gliomas belonged to other histologic classifications (Fig. 6a). This result was reinforced by the detection of *NEAT1* expression in 14 gliomas and 5 normal brains (Fig. 6b). After *NEAT1* was silenced by two different siRNAs (Fig. 6c), we found that the cell viability and proliferation were significantly inhibited in U87MG and U251 cells (Fig. 6d, e). Moreover, *NEAT1* knockdown induced a likewise G1 arrest as SRSF1 knockdown (Fig. 6f). Intracranial xenograft formation assay further verified that *NEAT1* was essential for glioma tumorigenesis, since *NEAT1* knockdown resulted in obviously growth retardation of the glioma xenografts (Supplementary Fig. 2). Therefore, we confirm that upregulated *NEAT1* is a growth promoter like SRSF1 by facilitating cell cycle progression in GBM cells.

3.5. SRSF1 facilitates G1 progression by elevating NEAT1-mediated cyclins and CDKs expression

Literature review implied that *NEAT1* was closely linked to cell cycle via positive regulation on expressions of cyclins and CDKs (Guo et al., 2018; Han et al., 2018; Wang et al., 2016). Correlation analysis indicated that multiple cell cycle-related genes (*E2F1*, *E2F2*, *MYBL2*, *CCND1*, *CDK2* and *CDK6*) had a significant positive correlation with *NEAT1* expression in Gene Expression Profiling Interactive Analysis

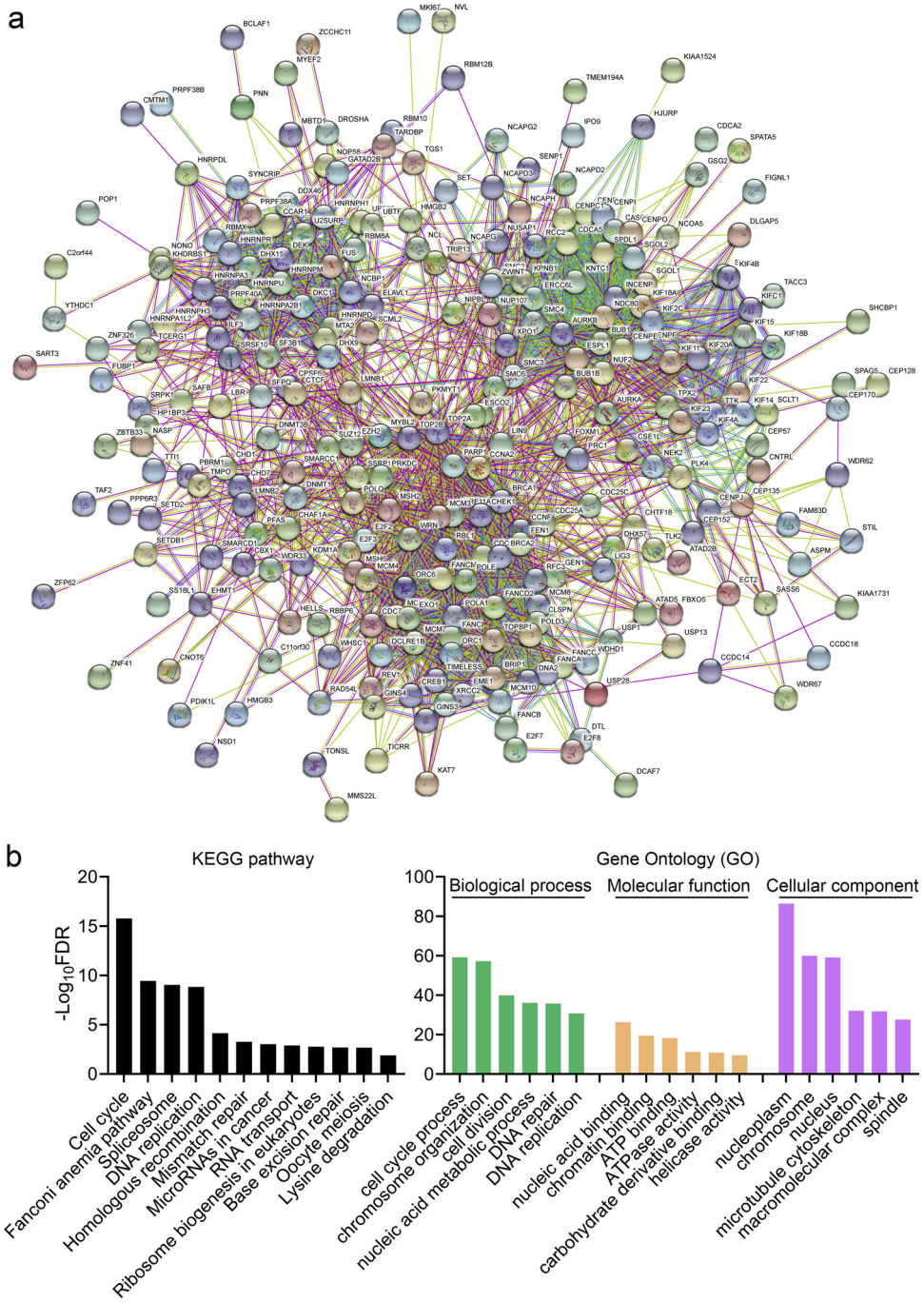

Fig. 2. *SRSF1*-co-expressed gene network indicates the involvement of SRSF1 in cell cycle regulation. (a) Protein-protein interaction network of *SRSF1*co-expressed genes screened by cBioportal and depicted by STRING. (b) KEGG pathway and GO enrichment analysis of *SRSF1*co-expressed genes by STRING. $-Log_{10}$ transformed false discovery rates (FDR) were plotted for each enriched functional category.

(GEPIA; http://gepia.cancer-pku.cn) dataset (Supplementary Fig. 3). Subsequently, qPCR confirmed that *NEAT1* knockdown led to downregulation of a panel of cell cycle-related genes in both U87MG and U251 cells (Supplementary Fig. 4a). Furthermore, Western blot showed that *NEAT1* knockdown resulted in decrease of Cyclin D1, Cyclin E2, CDK2 and CDK6 protein levels (Fig. 7a), keeping consistent with the above correlation analysis and qPCR results. Since the two complexes formed by Cyclin D1 and CDK6 (complex 1), and Cyclin E2 and CDK2 (complex2), are essential for cell transition from G1 phase to S phase, their lower levels are associated with G1 arrest and reduced growth rate (Malumbres and Barbacid, 2009). We also detected the expressions of these cell cycle-related genes in SRSF1-silenced GBM cells. The results came out the same downregulation of Cyclin D1, Cyclin E2 and CDK2 mRNA as well as protein levels upon SRSF1 knockdown (Supplementary Fig. 4b and Fig. 7b). Whereas for CDK6, SRSF1 knockdown merely downregulated its protein level (Supplementary Fig. 4b and Fig. 7b), implying the complexity of SRSF1 in regulating respective cell cycle-related gene. Nevertheless, both *NEAT1* knockdown and SRSF1 knockdown ultimately led to a profound expression inhibition on the G1/S transition protein complexes (Cyclin D1/CDK6, Cyclin E2/CDK2). Therefore, G1 arrest caused by *NEAT1* knockdown or SRSF1 knockdown could be explained by the decreased expressions of these cyclins and CDKs.

To confirm whether *NEAT1* is necessary for SRSF1-mediated cell

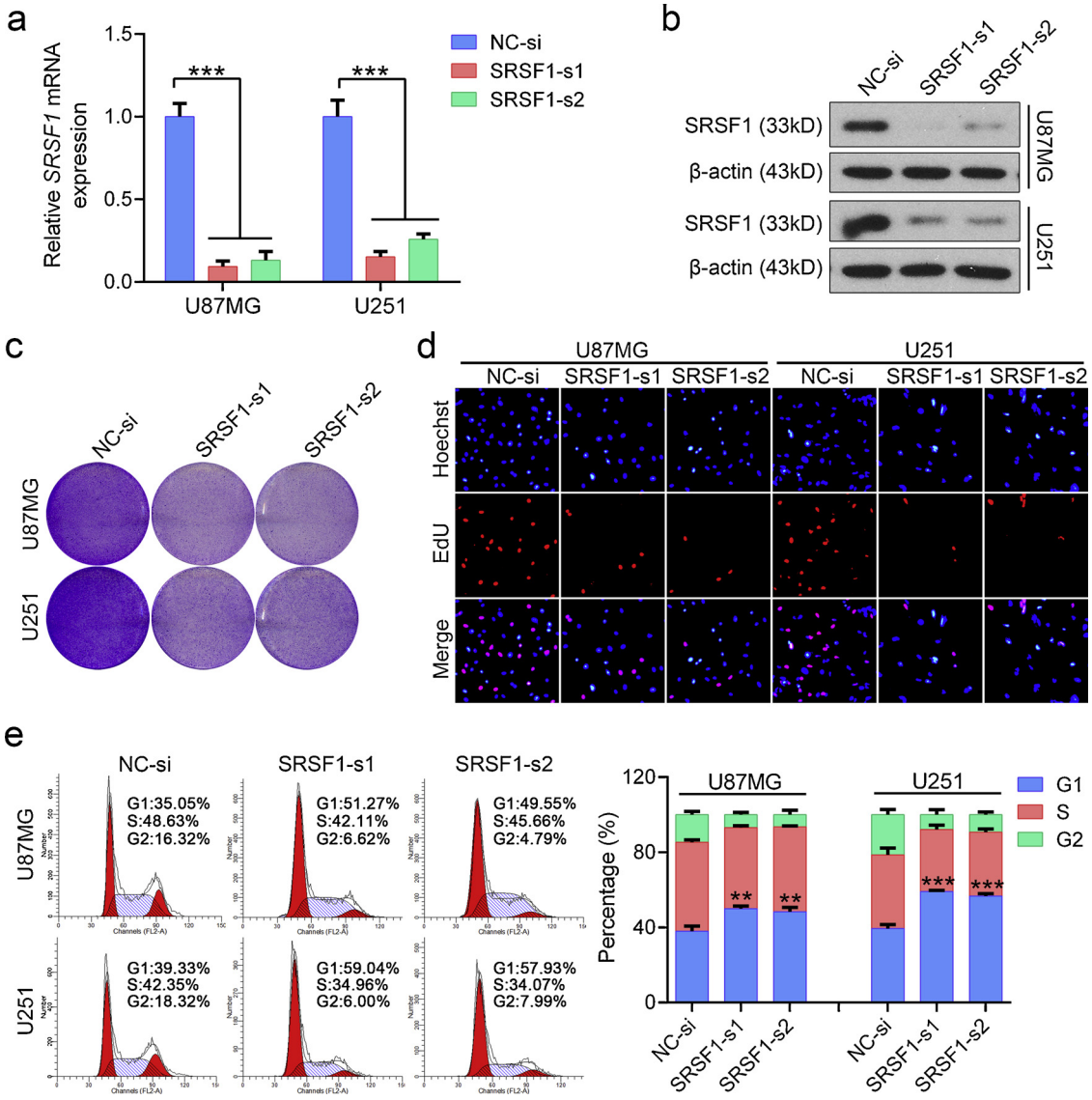

Fig. 3. Knockdown of SRSF1 inhibits GBM cell proliferation and cell cycle progression. (a) qPCR confirmation of SRSF1 knockdown in U87MG and U251cells transiently transfected with SRSF1siRNA (SRSF1-s1, SRSF1-s2) or negative control siRNA (NC-si). (b) Western blot confirmation of SRSF1 knockdown in U87MG and U251cells transfected as described in (a). Loading control: β-actin. (c) Cell viability revealed by crystal violet staining in U87MG and U251 cells transfected as described in (a). (d) Cell proliferation detected by EdU staining in U87MG and U251cells transfected as described in (a). (e) Cell cycle analyzed by flow cytometry in U87MG and U251cells transfected as described in (a). The left panel presents representative DNA content while the right shows the quantitative results. Data are presented as the mean ± SD. $^{**}P < 0.01$, $^{***}P < 0.001$.

cycle progression in GBM, we stably introduced *NEAT1_1* into SRSF1-sileced cells (sh-SRSF1 + *NEAT1*), and introduced the empty vector into control (sh-NC + vec) or SRSF1-sileced cells (sh-SRSF1 + vec) as the controls (Fig. 7c). In consistence with the above results, SRSF1 knockdown severely impaired the viability, proliferation and cell cycle, while *NEAT1* restoration significantly rescued the above defects (Fig. 7d–f). Moreover, *NEAT1* restoration also effectively abolished the suppressions of SRSF1-knockdown on the expressions of Cyclin D1, Cyclin E2, CDK2 and CDK6 (Fig. 7g). In vivo study revealed that *NEAT1* restoration significantly recovered the glioma tumorigenesis (Fig. 7h, i), further demonstrating the importance of *NEAT1* in mediating the growth promotion of SRSF1 in GBM cells.

3.6. *NEAT1 is associated with and stabilized by SRSF1*

The above findings clearly indicated that both SRSF1 and *NEAT1* promoted gliomagenesis via impacting on cell cycle, we then investigated the internal regulatory mechanism of *NEAT1* expression controlled by SRSF1 in GBM cells. Using the POSTAR2 database (http://lulab.life.tsinghua.edu.cn/postar) which integrated the human genome-scale maps of RBP-lncRNA interactions (Zhu et al., 2018), we predicted the potential *NEAT1_1*-interacted RBPs and found that SRSF1 was one of the RBPs binding with *NEAT1_1* (Fig. 8a). RIP lysates prepared from U87MG cells overexpressing HA-tagged SRSF1 were incubated with anti-HA tag antibody, and RT-PCR was performed to validate the *NEAT1* co-precipitation. As shown in Fig. 8b, the two endogenous *NEAT1* transcripts (*NEAT1_1* and *NEAT1_2*) were specifically associated with SRSF1 in GBM cells. Since human SRSF1 participates in several key aspects of mRNA metabolism including stability control (Das and Krainer, 2014), we next questioned whether SRSF1 regulated the stability of *NEAT1* in Actinomycin D (ActD)-treated GBM cells. When new *NEAT1* synthesis was blocked by ActD, SRSF1 knockdown resulted in a significant faster degradation of *NEAT1* level (Fig. 8c). Furthermore, we observed that *NEAT1* expression was positively correlated with SRSF1 both in our tissue samples (n = 19, Fig. 8d) and starBase-based 32 cancer types (http://starbase.sysu.edu.

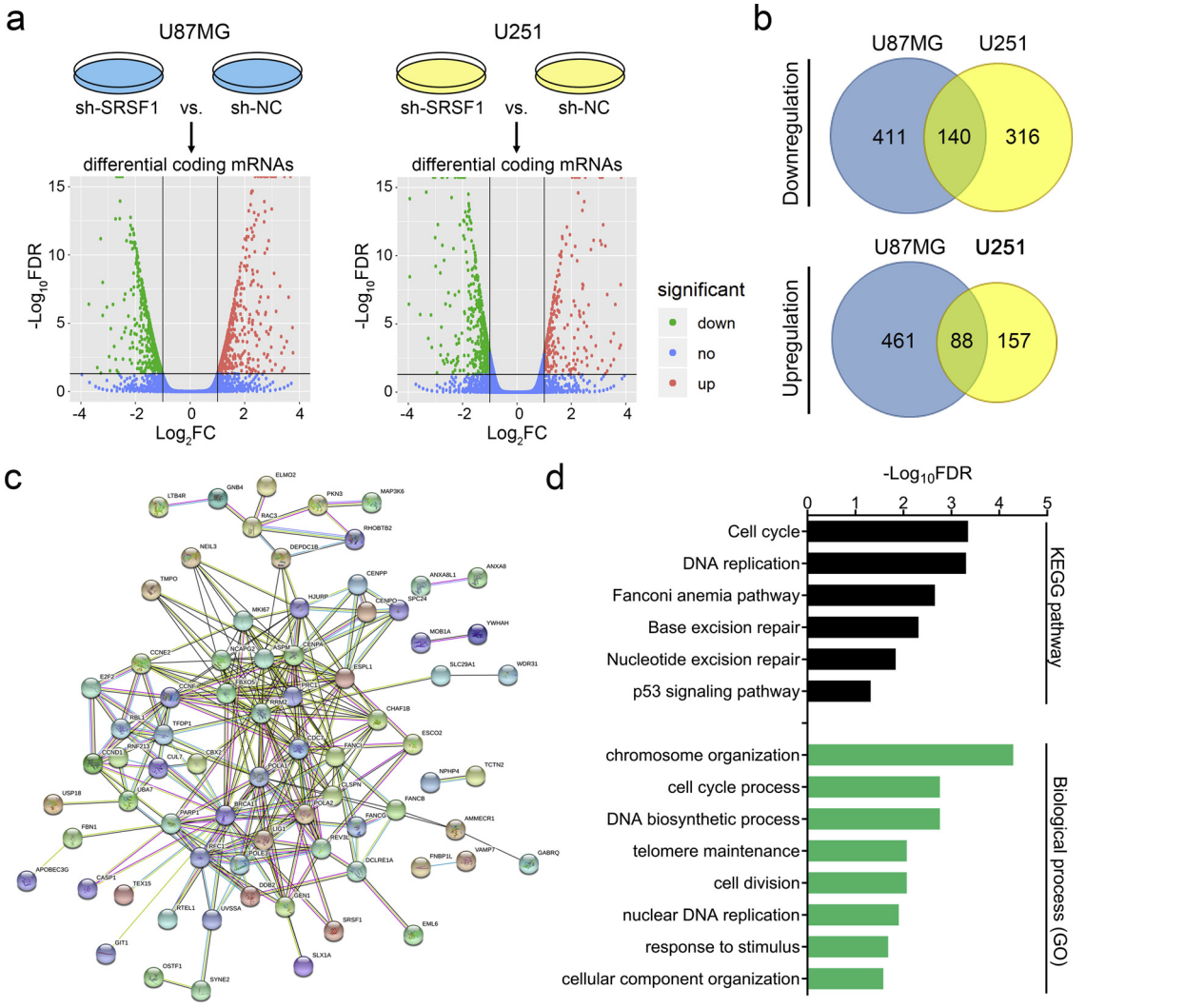

Fig. 4. Function annotation of the differential expressed coding gene affected by SRSF1 in GBM cells. (a) RNA-seq strategy and the volcano plots for the differential expressed coding mRNAs with fold change (FC) > 2 and FDR < 0.05. (b) Overlap of the downregulated or upregulated coding genes in U87MG and U251 cells affected by SRSF1 knockdown. (c) Functional association network of the overlapped SRSF1-activated coding genes depicted by STRING. (d) KEGG pathway and GO enrichment analysis of the overlapped SRSF1-activated coding genes by STRING. $-Log_{10}$ transformed FDR were plotted for each enriched functional category.

cn; Supplementary Table 4). In summary, these results demonstrated that SRSF1 could promote *NEAT1* expression by increasing its stability.

4. Discussion

Regulation of RNA metabolism (processing, transport, degradation and translation) is a key post-transcriptional modulation of gene expression that contributes to cancer development (Audic and Hartley, 2004). Our previous study clearly described the oncogenic roles of SRSF1 in gliomagenesis via AS control of *MYO1B* gene (Zhou et al., 2019). Through integrated data mining and experimental studies, we herein provide another interpretation of the oncogenic role of SRSF1 in gliomagenesis, that is, SRSF1 stabilizes lncRNA *NEAT1* to promote cell cycle progression and proliferation. Therefore, our findings indicate a splicing-independent mechanism of SRSF1 through regulating the stability/degradation of ncRNAs in glioma.

SRSF1, the most extensively characterized SR protein, is overexpressed in various tumors and exerts oncogenic functions (Das and Krainer, 2014). The linkage of SRSF1 with malignancy phenotypes mainly includes proliferation and motility promotion, and apoptosis inhibition (Das and Krainer, 2014; Ghigna et al., 2005; Karni et al., 2007). Recently, an insightful report of the SRSF1-affected translational landscape revealed its implication in cell cycle regulation (Maslon et al., 2014). Bioinformatics analysis of SRSF1-controled gene networks in colorectal cancer also implied that SRSF1 impacted on the expression of cell cycle-related genes (Sheng et al., 2017). Herein, we provided solid evidence that SRSF1 was indeed involved in cell cycle modulation: (1) *SRSF1*-co-expressed genes were markedly enriched in cell cycle regulation; (2) Knockdown of SRSF1 in two GBM cell lines resulted in significant G1 arrest and proliferation inhibition; (3) SRSF1-activated coding genes screened by RNA-seq were enriched in cell cycle control. Although numerous reports have identified the oncogenic functions of SRSF1 in human malignancies through AS regulation (Chen et al., 2017; Ghigna et al., 2005; Karni et al., 2007), we consider that some splicing-independent mechanisms also exist. Actually, in non-small cell lung cancer, SRSF1 could directly bind to *survivin* and *DNA ligase 1* (*LIG1*) mRNAs, increase their stabilities and enhance their translation in an mTOR-dependent manner (Ezponda et al., 2010; Martinez-Terroba et al., 2018).

Thanks to the high throughput RNA-seq technology, we could also screen out the poly-A-tailed ncRNAs affected by SRSF1. We observed that SRSF1 knockdown reduced *NEAT1* expression in U87MG and U251

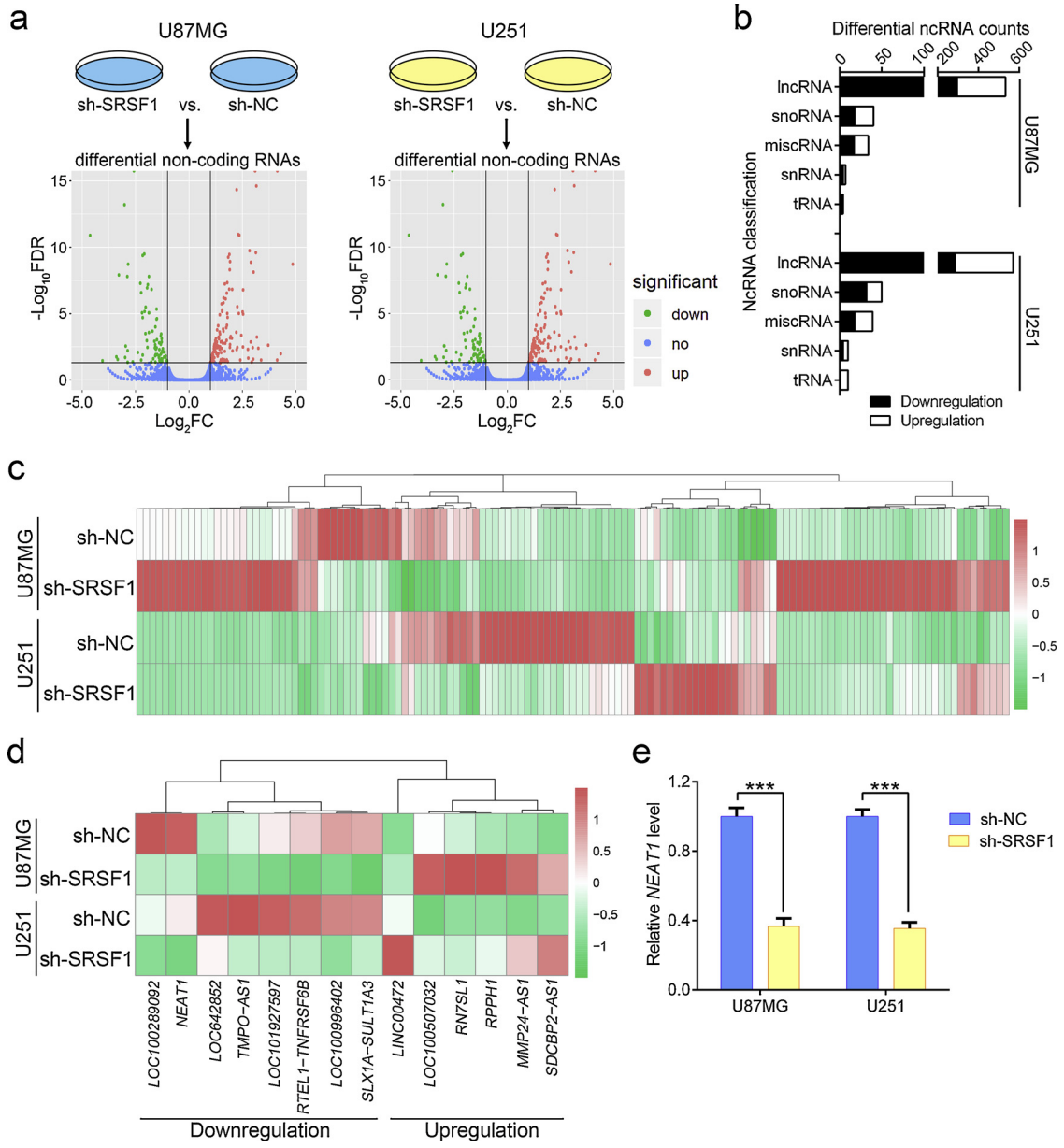

Fig. 5. Delving on the differential expressed ncRNAs impacted by SRSF1 knockdown in GBM cells. (a)Volcano plots for the differential expressed ncRNAs with FC > 2 and FDR < 0.05. (b) The statistics of each category of ncRNAs downregulated or upregulated by SRSF1 knockdown. (c) Heatmap of the differential expressed lncRNAs in U87MG and U251 cells affected by SRSF1 knockdown. (d) Heatmap of the overlapped differential expressed lncRNAs in U87MG and U251 cells affected by SRSF1 knockdown. (e) qPCR confirmation of *NEAT1* expression in SRSF1-silenced U87MG and U251 cells. Data are presented as the mean ± SD. ***$P < 0.001$.

cells. We then proved that like SRSF1, *NEAT1* was upregulated and could promote GBM cell proliferation by facilitating cell cycle progression in GBM cells. By way of *NEAT1* overexpression, we validated that *NEAT1* restoration could effectively rescued the impaired viability, proliferation and cell cycle progression due to SRSF1 knockdown. Protein levels of cyclins and CDKs exhibited the consistent alteration. Therefore, we identified *NEAT1* as an essential mediator of SRSF1's growth promotion activity in GBM cells.

As is known, *NEAT1*is a crucial oncogenic lncRNA in tumors (Klec et al., 2018; Zhou et al., 2018). Emerging studies have also suggested that *NEAT1* facilitates cell cycle progression and promotes expressions of cyclins and CDKs via microRNA (miRNA)-mediated competing endogenous RNA (ceRNA) mechanisms (Han et al., 2018; Huang et al., 2019; Wang et al., 2016; Wu et al., 2019; Yang et al., 2017; Zhang et al., 2017). For instance, the miR-193b-3p/CCND1 (in cervical cancer; Han et al., 2018), miR-377-3p/E2F3 (in lung cancer; Zhang et al., 2017), miR-107/CDK6 (in laryngeal cancer; Wang et al., 2016) axes have been connected with the pro-proliferation and pro-cell cycle progression activities of *NEAT1* in indicated cancers. However, in glioma, whether these ceRNA mechanisms exist, or any other axis takes the lead, remains unclear. Our correlation prediction revealed that *NEAT1* expression was positively correlated with that of *E2F1*, *E2F2*, *MYBL2*, *CCND1*, *CDK2* and *CDK6* genes. Therefore, we believe that there might be an upstream master cell cycle-related factor affected by *NEAT1*. Dissecting the landscape of RNA atlas controlled by *NEAT1* certainly benefits the comprehensive understanding of its role in gliomagenesis.

Concerning SRSF1, although its regulation on *NEAT1* stability is quite important for its pro-proliferation role in glioma, we consider that SRSF1 could impact on cell cycle control via other pathways, e.g. splicing and translation regulation. As is known, SRSF1 could modulate

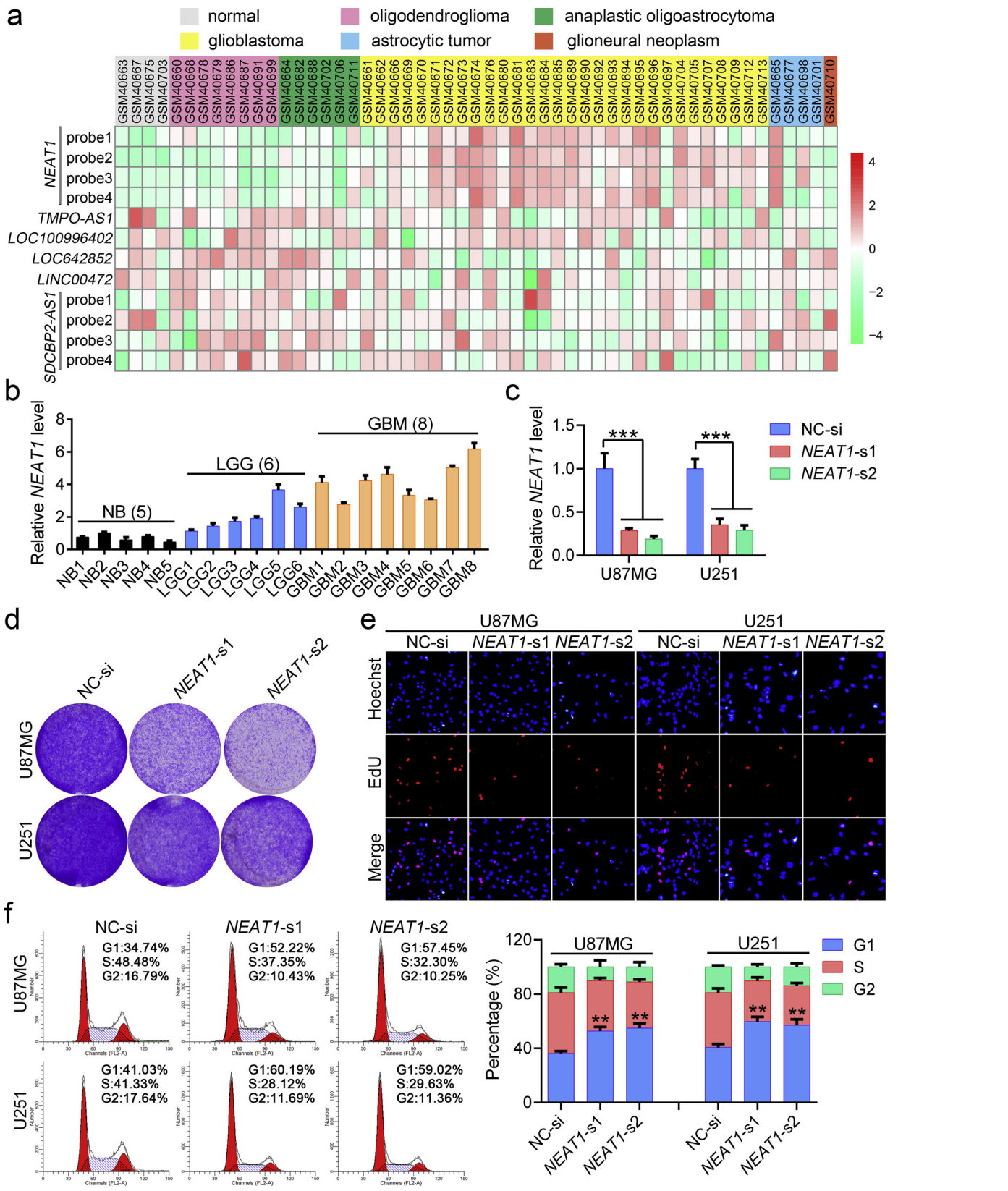

Fig. 6. Increased *NEAT1* in GBM promotes cell proliferation and cell cycle progression. (a) Heatmap of the overlapped differential expressed lncRNAs in a glioma dataset grouped by histopathology. (b) qPCR detection of *NEAT1* levels in normal brains (NBs, n = 5), low grade gliomas (LGGs, n = 6) and GBMs (n = 8). (c) qPCR confirmation of *NEAT1* knockdown in U87MG and U251cells transiently transfected with *NEAT1* siRNA (*NEAT1*-s1, *NEAT1*-s2) or negative control siRNA (NC-si). (d) Cell viability revealed by crystal violet staining in U87MG and U251 cells transfected as described in (c). (e) Cell proliferation detected by EdU staining in U87MG and U251cells transfected as described in (c). (f) Cell cycle analyzed by flow cytometry in U87MG and U251cells transfected as described in (c). The left panel presents representative DNA content while the right shows the quantitative results. Data are presented as the mean ± SD. $^{**}P < 0.01$, $^{***}P < 0.001$.

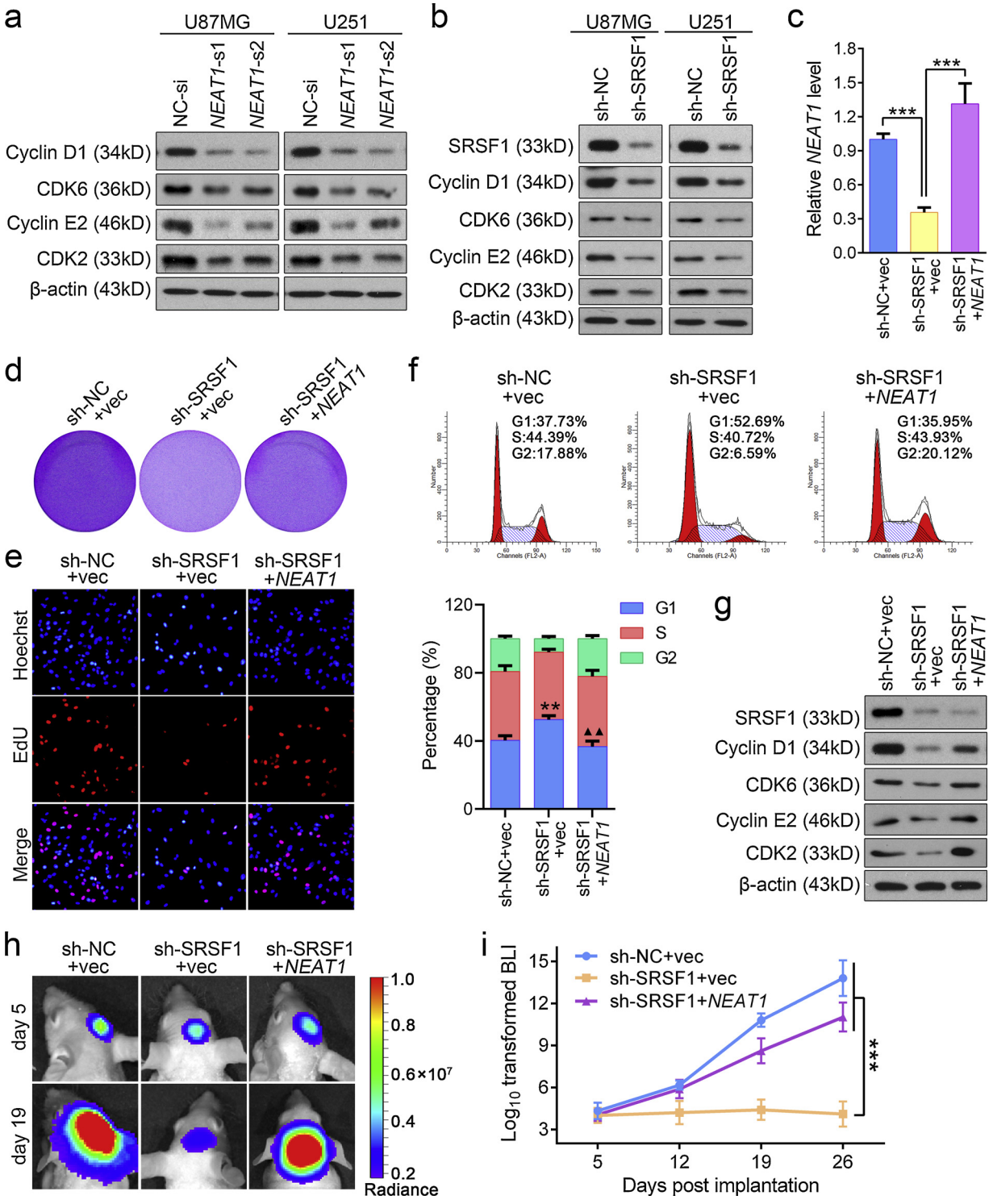

Fig. 7. SRSF1 facilitates G1 progression by elevating *NEAT1*-mediated cyclins and CDKs expression. (a) Western blot of G1-related cyclins and CDKs in U87MG and U251cells transfected as described in Fig. 6c. (b) Western blot of G1-related cyclins and CDKs in SRSF-silenced U87MG and U251cells. (c) qPCR detection of *NEAT1* expression in SRSF1-silenced U87MG cells stably transfected with the *NEAT1* plasmid. (d) Cell viability revealed by crystal violet staining in U87MG cells treated as described in (c). (e) Cell proliferation detected by EdU staining in U87MG cells treated as described in (c). (f) Cell cycle analyzed by flow cytometry in U87MG cells treated as described in (c). The upper panel presents representative DNA content while the bottom shows the quantitative results. (g) Western blot of G1-related cyclins and CDKs in U87MG cells treated as described in (c). (h) Bioluminescence images of the intracranial glioma xenografts formed by the indicated U87MG cells. Images of representative mice are shown. (i) Bioluminescence quantification results at day 5, 12, 19 and 26 after implantation (n = 6 for each group). Data are presented as the mean ± SD. $^{**}P < 0.01$, $^{***}P < 0.001$.

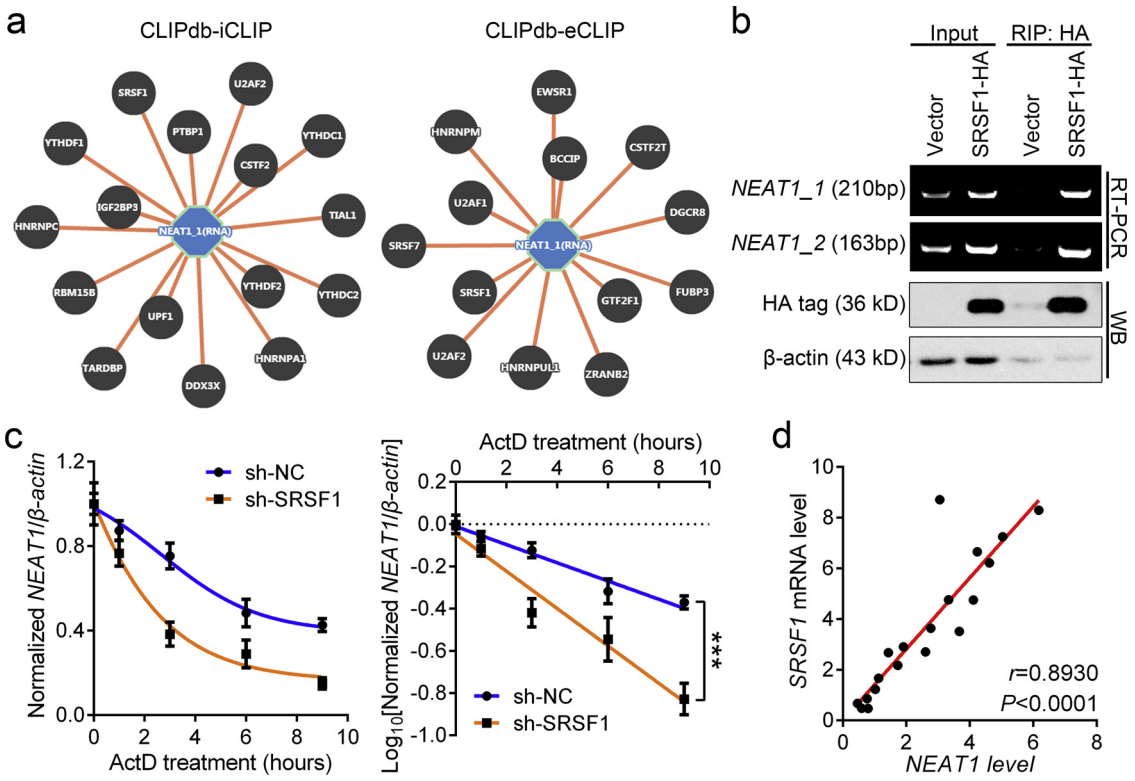

Fig. 8. *NEAT1* is associated with and stabilized by SRSF1. (a) Prediction of potential *NEAT1_1*-interacted RBPs by using the POSTAR2 database. (b) Upper: Directly binding between SRSF1 and endogenous *NEAT1* fragments verified by RT-PCR. Bottom: Western blot confirmation of SRSF1 overexpression in U87MG cells. Loading control: β-actin. (c) Comparison of *NEAT1* degradation between control (sh-NC) and SRSF1-silenced (sh-SRSF1) cells in which *NEAT1* synthesis was interdicted with ActD (5 μg/mL). Densitometry *NEAT1* values were normalized for each time point with β-actin (left) and $\log_{10}$ transformed values were used to statistically compare growth slopes (right). Data are presented as the mean ± SD. ***$P < 0.001$. (d) Pearson correlation analysis between *SRSF1* and *NEAT1* levels in normal brains and gliomas (n = 19). Pearson correlation test, r and P values are shown.

the AS on *MYB* and *MYBL2*, two proto-oncogenes (transcription factors) involved in cell cycle progression (Karni et al., 2007). Besides, SRSF1 could promote the translation of genes associated with cell cycle and cell division, which could partially explain the oncogenic role of SRSF1 in cancer (Maslon et al., 2014). Therefore, SRSF1 exerts complex activities in controlling gene expression. This could be reflected by the downregulation of CDK6 protein while no change of *CDK6* mRNA in SRSF1-silenced GBM cells.

Recently, a study from ovarian cancer demonstrated that *NEAT1* was stabilized by the RBP HuR and contributed to ovarian carcinogenesis (Chai et al., 2016). It was the first causality report illustrating the regulation of *NEAT1* stability by RBPs. Our findings on the one hand fill the gaps on the splicing-independent mechanisms of SRSF1 in gliomagenesis, on the other hand identify *NEAT1* also as a target of SRSF1 through stability control, indicating that lncRNA stability control by RBP is not an exception and deserves more attention in future.

5. Conclusion

In summary, we demonstrate that SRSF1 and lncRNA *NEAT1* both are upregulated in glioma. Through binding to and stabilizing *NEAT1*, SRSF1 enhances *NEAT1* expression and facilitates GBM cell proliferation via cell cycle control. Our results provide novel insights on the splicing-independent mechanisms of SRSF1 in glioma, and confirm SRSF1 as a supervisor of *NEAT1* RNA stability. Both SRSF1 and *NEAT1* may serve as promising targets for future glioma therapy.

Author contributions

X.Z., X.L., L.Y., R.W., S.Y. contributed to experimental design and performed experiments; D.H., C.S., C.S., W.L., C.R., Z.J. provided FFPE samples and the pathological characterization of glioma samples; X.Z., X.L., L.Y., R.W., Q.W., S.Y. analyzed the data; X.Z., S.Y. wrote the manuscript.

Competing financial interest

The authors declare no competing financial interests.

Acknowledgement

This study was supported by grants from the National Natural Science Foundation of China (No. 81302002, 81402050, 81502166, 81672592 and 81872061), the Programs of Science and Technology Commission Foundation of Tianjin Municipality (No. 16JCQNJC13400, 17JCYBJC27100 and 18JCYBJC92100), the Program of Tianjin Municipal Health Bureau (No. 15KJ147), the Foundation of Tianjin Medical University and General Hospital (No. 2015KYZQ11 and ZYYFY2015032), and the “New Century” Talent Training Project of TMUGH (2016, to Xuexia Zhou).

Appendix A. Supplementary data

Supplementary material related to this article can be found, in the online version, at doi:https://doi.org/10.1016/j.biocel.2019.06.003.

References

Alexander, B.M., Cloughesy, T.F., 2017. Adult glioblastoma. J. Clin. Oncol. 35 (21), 2402–2409.
Audic, Y., Hartley, R.S., 2004. Post-transcriptional regulation in cancer. Biol. Cell 96 (7), 479–498.
Balas, M.M., Johnson, A.M., 2018. Exploring the mechanisms behind long noncoding

RNAs and cancer. Noncoding RNA Res. 3 (3), 108–117.
Besson, A., Yong, V.W., 2001. Mitogenic signaling and the relationship to cell cycle regulation in astrocytomas. J. Neurooncol. 51 (3), 245–264.
Bredel, M., Bredel, C., Juric, D., Duran, G.E., Yu, R.X., Harsh, G.R., Vogel, H., Recht, L.D., Scheck, A.C., Sikic, B.I., 2006. Tumor necrosis factor-alpha-induced protein 3 as a putative regulator of nuclear factor-kappaB-mediated resistance to O6-alkylating agents in human glioblastomas. J. Clin. Oncol. 24 (2), 274–287.
Castello, A., Fischer, B., Eichelbaum, K., Horos, R., Beckmann, B.M., Strein, C., Davey, N.E., Humphreys, D.T., Preiss, T., Steinmetz, L.M., Krijgsveld, J., Hentze, M.W., 2012. Insights into RNA biology from an atlas of mammalian mRNA-binding proteins. Cell 149 (6), 1393–1406.
Chai, Y., Liu, J., Zhang, Z., Liu, L., 2016. HuR-regulated lncRNA NEAT1 stability in tumorigenesis and progression of ovarian cancer. Cancer Med. 5 (7), 1588–1598.
Chen, L., Luo, C., Shen, L., Liu, Y., Wang, Q., Zhang, C., Guo, R., Zhang, Y., Xie, Z., Wei, N., Wu, W., Han, J., Feng, Y., 2017. SRSF1 prevents DNA damage and promotes tumorigenesis through regulation of DBF4B Pre-mRNA splicing. Cell Rep. 21 (12), 3406–3413.
Conlon, E.G., Manley, J.L., 2017. RNA-binding proteins in neurodegeneration: mechanisms in aggregate. Genes Dev. 31 (15), 1509–1528.
Das, S., Krainer, A.R., 2014. Emerging functions of SRSF1, splicing factor and oncoprotein, in RNA metabolism and cancer. Mol. Cancer Res. 12 (9), 1195–1204.
Evan, G.I., Vousden, K.H., 2001. Proliferation, cell cycle and apoptosis in cancer. Nature 411 (6835), 342–348.
Ezponda, T., Pajares, M.J., Agorreta, J., Echeveste, J.I., Lopez-Picazo, J.M., Torre, W., Pio, R., Montuenga, L.M., 2010. The oncoprotein SF2/ASF promotes non-small cell lung cancer survival by enhancing survivin expression. Clin. Cancer Res. 16 (16), 4113–4125.
Ghigna, C., Giordano, S., Shen, H., Benvenuto, F., Castiglioni, F., Comoglio, P.M., Green, M.R., Riva, S., Biamonti, G., 2005. Cell motility is controlled by SF2/ASF through alternative splicing of the Ron protooncogene. Mol. Cell 20 (6), 881–890.
Guo, H.M., Yang, S.H., Zhao, S.Z., Li, L., Yan, M.T., Fan, M.C., 2018. LncRNA NEAT1 regulates cervical carcinoma proliferation and invasion by targeting AKT/PI3K. Eur. Rev. Med. Pharmacol. Sci. 22 (13), 4090–4097.
Han, D., Wang, J., Cheng, G., 2018. LncRNA NEAT1 enhances the radio-resistance of cervical cancer via miR-193b-3p/CCND1 axis. Oncotarget 9 (2), 2395–2409.
Hong, S., 2017. RNA binding protein as an emerging therapeutic target for Cancer prevention and treatment. J. Cancer Prev. 22 (4), 203–210.
Hruz, T., Laule, O., Szabo, G., Wessendorp, F., Bleuler, S., Oertle, L., Widmayer, P., Gruissem, W., Zimmermann, P., 2008. Genevestigator v3: a reference expression database for the meta-analysis of transcriptomes. Adv. Bioinformatics 2008, 420747.
Huang, X., Zhong, R., He, X., Deng, Q., Peng, X., Li, J., Luo, X., 2019. Investigations on the mechanism of progesterone in inhibiting endometrial cancer cell cycle and viability via regulation of long noncoding RNA NEAT1/microRNA-146b-5p mediated Wnt/beta-catenin signaling. IUBMB Life 71 (2), 223–234.
Karni, R., de Stanchina, E., Lowe, S.W., Sinha, R., Mu, D., Krainer, A.R., 2007. The gene encoding the splicing factor SF2/ASF is a proto-oncogene. Nat. Struct. Mol. Biol. 14 (3), 185–193.
Klec, C., Prinz, F., Pichler, M., 2018. Involvement of the long noncoding RNA NEAT1 in carcinogenesis. Mol. Oncol. 13 (1), 46–60.
Lara-Velazquez, M., Al-Kharboosh, R., Jeanneret, S., Vazquez-Ramos, C., Mahato, D., Tavanaiepour, D., Rahmathulla, G., Quinones-Hinojosa, A., 2017. Advances in brain tumor surgery for glioblastoma in adults. Brain Sci. 7 (12).
Li, H., Yu, L., Liu, J., Bian, X., Shi, C., Sun, C., Zhou, X., Wen, Y., Hua, D., Zhao, S., Ren, L., An, T., Luo, W., Wang, Q., Yu, S., 2017a. miR-320a functions as a suppressor for gliomas by targeting SND1 and beta-catenin, and predicts the prognosis of patients. Oncotarget 8 (12), 19723–19737.
Li, X., Zhou, X., Li, Y., Zu, L., Pan, H., Liu, B., Shen, W., Fan, Y., Zhou, Q., 2017b. Activating transcription factor 3 promotes malignance of lung cancer cells in vitro. Thorac. Cancer 8 (3), 181–191.
Liu, J., Xu, J., Li, H., Sun, C., Yu, L., Li, Y., Shi, C., Zhou, X., Bian, X., Ping, Y., Wen, Y., Zhao, S., Xu, H., Ren, L., An, T., Wang, Q., Yu, S., 2015. miR-146b-5p functions as a tumor suppressor by targeting TRAF6 and predicts the prognosis of human gliomas. Oncotarget 6 (30), 29129–29142.
Louis, D.N., Perry, A., Reifenberger, G., von Deimling, A., Figarella-Branger, D., Cavenee, W.K., Ohgaki, H., Wiestler, O.D., Kleihues, P., Ellison, D.W., 2016. The 2016 world health organization classification of tumors of the central nervous system: a summary. Acta Neuropathol. 131 (6), 803–820.
Malumbres, M., Barbacid, M., 2009. Cell cycle, CDKs and cancer: a changing paradigm. Nat. Rev. Cancer 9 (3), 153–166.
Martinez-Terroba, E., Ezponda, T., Bertolo, C., Sainz, C., Remirez, A., Agorreta, J., Garmendia, I., Behrens, C., Pio, R., Wistuba, I.I., Montuenga, L.M., Pajares, M.J., 2018. The oncogenic RNA-binding protein SRSF1 regulates LIG1 in non-small cell lung cancer. Lab. Invest. 98 (12), 1562–1574.
Maslon, M.M., Heras, S.R., Bellora, N., Eyras, E., Caceres, J.F., 2014. The translational landscape of the splicing factor SRSF1 and its role in mitosis. Elife, e02028.
Masuda, K., Kuwano, Y., 2018. Diverse roles of RNA-binding proteins in cancer traits and their implications in gastrointestinal cancers. Wiley Interdiscip. Rev. RNA e1520.
Moore, K.S., von Lindern, M., 2018. RNA binding proteins and regulation of mRNA translation in Erythropoiesis. Front. Physiol. 9, 910.
Peng, Z., Liu, C., Wu, M., 2018. New insights into long noncoding RNAs and their roles in glioma. Mol. Cancer 17 (1), 61.
Pereira, B., Billaud, M., Almeida, R., 2017. RNA-binding proteins in Cancer: old players and new actors. Trends Cancer 3 (7), 506–528.
Rafiee, A., Riazi-Rad, F., Havaskary, M., Nuri, F., 2018. Long noncoding RNAs: regulation, function and cancer. Biotechnol. Genet. Eng. Rev. 34 (2), 153–180.
Sheng, J., Zhao, J., Xu, Q., Wang, L., Zhang, W., Zhang, Y., 2017. Bioinformatics analysis of SRSF1-controlled gene networks in colorectal cancer. Oncol. Lett. 14 (5), 5393–5399.
Shi, J., Dong, B., Cao, J., Mao, Y., Guan, W., Peng, Y., Wang, S., 2017. Long non-coding RNA in glioma: signaling pathways. Oncotarget 8 (16), 27582–27592.
Wang, P., Wu, T., Zhou, H., Jin, Q., He, G., Yu, H., Xuan, L., Wang, X., Tian, L., Sun, Y., Liu, M., Qu, L., 2016. Long noncoding RNA NEAT1 promotes laryngeal squamous cell cancer through regulating miR-107/CDK6 pathway. J. Exp. Clin. Cancer Res. 35, 22.
Wu, D.M., Wang, S., Wen, X., Han, X.R., Wang, Y.J., Fan, S.H., Zhang, Z.F., Shan, Q., Lu, J., Zheng, Y.L., 2019. Long noncoding RNA nuclear enriched abundant transcript 1 impacts cell proliferation, invasion, and migration of glioma through regulating miR-139-5p/ CDK6. J. Cell. Physiol. 234 (5), 5972–5987.
Yang, X., Xiao, Z., Du, X., Huang, L., Du, G., 2017. Silencing of the long non-coding RNA NEAT1 suppresses glioma stem-like properties through modulation of the miR-107/CDK6 pathway. Oncol. Rep. 37 (1), 555–562.
Zhang, J., Li, Y., Dong, M., Wu, D., 2017. Long non-coding RNA NEAT1 regulates E2F3 expression by competitively binding to miR-377 in non-small cell lung cancer. Oncol. Lett. 14 (4), 4983–4988.
Zhou, K., Zhang, C., Yao, H., Zhang, X., Zhou, Y., Che, Y., Huang, Y., 2018. Knockdown of long non-coding RNA NEAT1 inhibits glioma cell migration and invasion via modulation of SOX2 targeted by miR-132. Mol. Cancer 17 (1), 105.
Zhou, X., Li, X., Cheng, Y., Wu, W., Xie, Z., Xi, Q., Han, J., Wu, G., Fang, J., Feng, Y., 2014a. BCLAF1 and its splicing regulator SRSF10 regulate the tumorigenic potential of colon cancer cells. Nat. Commun. 5, 4581.
Zhou, X., Li, X., Sun, C., Shi, C., Hua, D., Yu, L., Wen, Y., Hua, F., Wang, Q., Zhou, Q., Yu, S., 2017. Quaking-5 suppresses aggressiveness of lung cancer cells through inhibiting beta-catenin signaling pathway. Oncotarget 8 (47), 82174–82184.
Zhou, X., Wang, R., Li, X., Yu, L., Hua, D., Sun, C., Shi, C., Luo, W., Rao, C., Jiang, Z., Feng, Y., Wang, Q., Yu, S., 2019. Splicing factor SRSF1 promotes gliomagenesis via oncogenic splice-switching of MYO1B. J. Clin. Invest. 129 (2), 676–693.
Zhou, X., Wu, W., Li, H., Cheng, Y., Wei, N., Zong, J., Feng, X., Xie, Z., Chen, D., Manley, J.L., Wang, H., Feng, Y., 2014b. Transcriptome analysis of alternative splicing events regulated by SRSF10 reveals position-dependent splicing modulation. Nucleic Acids Res. 42 (6), 4019–4030.
Zhu, Y., Xu, G., Yang, Y.T., Xu, Z., Chen, X., Shi, B., Xie, D., Lu, Z.J., Wang, P., 2018. POSTAR2: deciphering the post-transcriptional regulatory logics. Nucleic Acids Res. 47 (1), 203–211.